Anticyclonic Lenses in Large-Scale Strain and Shear

BARRY R. RUDDICK

Department of Oceanography, Dalhousie University, Halifax, N.S., B3H4J1 Canada

(Manuscript received 21 March 1986, in final form 30 October 1986)

ABSTRACT

A three-layer model is used to study the effects of pure strain flow and simple shearing flow on isolated, anticyclonic, baroclinic vortices such as Mediterranean salt lenses. Exact steady solutions are found representing elliptical vortices with uniform interior vorticity. These solutions become increasingly elliptical with increasing strain or shear, with the major axis always 45° clockwise from the principal (outflow) axis of the strain field. This is shown to be necessary so that the mean flow not exchange energy with the lens. At some critical value of strain or shear, these solutions cease to exist. The results suggest that for a lens of a given Rossby number, there is a maximum large-scale strain beyond which the lens must undergo drastic changes in order to survive.

The geostrophic adjustment of an infinitely long strip aligned with a simple shearing flow is also investigated. It is found that the shear modifies the distance of outward adjustment, but not the profile of the adjusted region. The strong flow and vorticity near the edge, and the assumed infinite length, allow the strip to persist in environmental shear as strong as f, the Coriolis parameter.

1. Introduction

Lenses of strongly anomalous water, isolated from the sea surface and bottom and rotating anticyclonically, have been observed in several locations of the world's oceans. McDowell and Rossby (1978) observed a "Meddy," a lens of Mediterranean Water, near the Bahamas. Armi and Zenk (1985) report on three such lenses discovered in the Canary Basin, nearer the presumed source. These lenses were 500–800 m thick in the center and were roughly circular with a radius of 30–50 km, which is several baroclinic deformation radii. Their salinity anomaly is very strong—many standard deviations from the mean temperature–salinity (T–S) curve. Because they are spawned in the eastern Atlantic, and at least some manage to migrate to the west, they may collectively play an important role in the along-isopycnal transport of heat and salt. The changes of a lens surviving various instabilities, dissipative processes, and other interactions will, of course, affect these transports.

During their migrations, these lenses are embedded in the larger-scale mesoscale eddy field. The velocity and vorticity of the eddy field will advect and rotate the lens. The strain field attempts to distort the lens from circular symmetry, and perhaps even tear it apart if it is strong enough or if the lens is too large. As Rossby (1982) says,

> This strength (high velocity) and the small size of these features may give us a clue as to why they are long-lived: if the horizontal shear of the background flow were strong enough, a large (lens) could be stretched apart in a cascade to smaller and smaller scales. . . . This may help to explain why no very large Mediterranean eddies have been observed: they suffer a violent death!

In this paper, the effect of a large-scale strain or a uniform shear on a lens is investigated using a three-layer model. We find steady lenslike solutions with uniform interior vorticity, valid for finite lens Rossby number and finite mean flow strength. These solutions cease to exist for strong environmental velocity gradients.

There is little previous related work on the behavior of isolated vortices in sheared or strained environments. Moore and Saffman (1971) found an exact solution for an inviscid, barotropic elliptical vortex in uniform irrotational strain, α, in a nonrotating fluid. Their findings are similar to ours, predicting a critical strain beyond which the solution does not exist. In a fairly comprehensive review of isolated lenses, McWilliams (1985) showed that the potential vorticity gradients in the neighborhood of a fluid parcel would tend not to grow, and so allow the lens to remain coherent, when the local lens vorticity is greater than the large-scale strain. This condition also allows fluid parcels to be trapped within the lens:

$$\omega_0^2 > \alpha^2. \tag{1.1}$$

Nof (1985) investigated the ellipticity of isolated lenses in a simple shearing flow, finding that they become more elliptical as the strength of the shear increases. We extend this work to finite Rossby number and to pure straining motions and find that there are limits to the magnitude of the environmental strain/shear that allow steady solutions of the postulated form to exist,

and that cyclonic and anticyclonic shear affect the lens differently.

In section 2, the three-layer reduced-gravity model for baroclinic lenses is set out, allowing for environmental velocities. In section 3, some integral constraints on the layer are deduced. In section 4 elliptical lenses in a strain are studied, and in section 5 we study elliptical lenses in simple shear. The geostrophic adjustment of a long strip in simple shear is solved in section 6, and the results are summarized and discussed in section 7.

2. Formulation

We choose a three-layer model with velocities $\tilde{u}_i = (u_i, v_i, w_i)$, densities ρ_i, and pressures p_i in each layer. We constrain the velocities in layers 1 (top) and 3 (bottom) to both be equal to the prescribed mean flow $(\bar{u}, \bar{v}, 0)$, which can be either a pure strain field (sections 3 and 4) or a simple shear (sections 5 and 6). Prescribing the external flow has the effect of assuming that the top and bottom layers are infinitely deep compared to the lens, so that the lens has no back effect on the mean flow. Assuming equal velocities, and thus equal pressure gradient forces, in these layers leads to the condition

$$\eta_2 = \eta_1\left[\frac{\rho_2-\rho_1}{\rho_3-\rho_2}\right] \tag{2.1}$$

where η_1 and η_2 are the displacements of the upper and lower interfaces of the lens, as shown in Fig. 1. We define $h(x, y, t) = \eta_1 + \eta_2$, the thickness of the lens. Under the Boussinesq and hydrostatic assumptions, and dropping the subscript 2, the equations of motion for the lens (layer 2) are

$$\frac{du}{dt} - fv = -g'\frac{\partial h}{\partial x} + \left(\frac{d\bar{u}}{dt} - f\bar{v}\right) \tag{2.2}$$

$$\frac{dv}{dt} + fu = -g'\frac{\partial h}{\partial y} + \left(\frac{d\bar{v}}{dt} + f\bar{u}\right) \tag{2.3}$$

$$\frac{dh}{dt} + h\left(\frac{\partial u}{\partial x} + \frac{\partial v}{\partial y}\right) = 0 \tag{2.4}$$

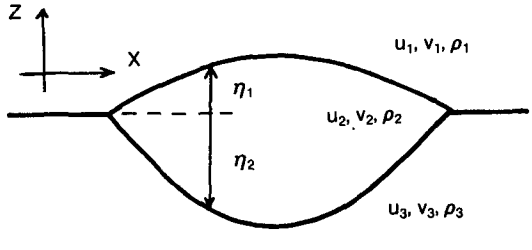

FIG. 1. Sketch of the lens model used, showing the three layers $i = 1, 2, 3$. The central layer is assumed here to be of finite horizontal extent.

where the reduced gravity is

$$g' = g\left(\frac{\rho_3-\rho_1}{\rho_3}\right)(1-a)a \tag{2.5}$$

$$a = \frac{\rho_2-\rho_1}{\rho_3-\rho_1}.$$

For equal density jumps at the upper and lower interfaces, $a = \frac{1}{2}$. The usual two-layer formulation used for Gulf Stream rings is recovered by letting $\rho_1 = 0$.

The equations of motion for layers 1 and 3 show that the bracketed terms in (2.2) and (2.3) are the pressure gradient forces of the mean flow. Thus, the coupling between the central lens layer and the upper and lower layers is only via pressure forces. Since these can transmit no torques, an immediate conclusion is that the potential vorticity of each fluid column of the lens is conserved. [This can be demonstrated by cross-differentiating (2.2) and (2.3) and using the equations of motion for the upper layer.] This constraint can only be broken if the layers are coupled via friction or mixing.

3. Steady strain field—integral theorems

In this section we assume that the lens is of finite horizontal extent, as shown in Fig. 1, and that the mean velocity is a uniform steady strain, with principal axes at 45° to the x-axis:

$$\bar{u} = \alpha y \tag{3.1}$$

$$\bar{v} = \alpha x. \tag{3.2}$$

The equations of motion for the lens (2.2)–(2.4) become

$$\frac{du}{dt} - fv = -g'\frac{\partial h}{\partial x} + (\alpha^2 - \alpha f)x \tag{3.3}$$

$$\frac{dv}{dt} + fu = -g'\frac{\partial h}{\partial y} + (\alpha^2 + \alpha f)y \tag{3.4}$$

$$\frac{dh}{dt} + h\left(\frac{\partial u}{\partial x} + \frac{\partial v}{\partial y}\right) = 0. \tag{3.5}$$

These are just the shallow water equations with forcing terms proportional to x and y. In the following we assume that the lens thickness goes to zero at finite radius.

Conservation of potential vorticity for the lens can be demonstrated by differentiating (3.3) by y, (3.4) by x, subtracting, and using (3.5) to obtain

$$\frac{d}{dt}\left(\frac{f + \partial v/\partial x - \partial u/\partial y}{h}\right) = 0. \tag{3.6}$$

Integrating (3.5) over the area of the lens and using the divergence theorem gives

$$\frac{\partial}{\partial t}\int\int h\,dx\,dy = 0, \tag{3.7}$$

which states that the volume of the lens remains constant.

To form an energy equation for the lens, we multiply (3.3) by hu, (3.4) by hv, and after some manipulation (see p. 67 of Pedlosky, 1979), we obtain

$$\frac{\partial}{\partial t}[h(u^2+v^2)/2+g'h^2/2]+\nabla_H\cdot\{hu[g'h+(u^2+v^2)/2]\}$$
$$=(\alpha^2-\alpha f)uhx+(\alpha^2+\alpha f)vhy. \quad (3.8)$$

This is then integrated over the area of the lens, eliminating the second term to obtain

$$\frac{\partial}{\partial t}\int\int\{h(u^2+v^2)/2+g'h^2/2\}dxdy$$
$$=\int\int\{(\alpha^2-\alpha f)xhu+(\alpha^2+\alpha f)yhv\}dxdy. \quad (3.9)$$

The left side is identified with the kinetic and potential energies of the lens; the right side expresses the work done on the lens by the mean flow in layers 1 and 3.

Since there is no dissipation in the model, steady solutions can only be obtained if the rhs of (3.9) is zero. One obvious way this can occur is if h = constant and $u = \alpha y$, $v = \alpha x$, corresponding to a barotropic flow. Even though the central layer is of infinite extent, there is no energy exchange in this case.

Another way that no energy exchange can occur is if the central layer has a lenslike disturbance with axes of symmetry along the x- and y-axes. In this case, h is symmetric in both x and y, u is symmetric in x and antisymmetric in y, and v is symmetric in y but antisymmetric in x. Each term on the rhs of (3.9) is antisymmetric in both x and y, so the integral is zero. One class of lenses satisfying this symmetry property is an elliptical lens with the major axis along either the x- or y-axis (section 4), at 45° to the principal strain axis. An example is sketched in Fig. 2.

For a barotropic vortex in a nonrotating strain field, Moore and Saffman (1971) found that the steady solution was elliptical, with the major axis at 45° to the principal strain axis. They explain this result in terms of the pressure at the rim, but a more appealing explanation in terms of energy exchange, analogous to (3.9), is possible. Tennekes and Lumley (1972, p. 63) show that the work done on a turbulent velocity field by a mean flow is given by the product of the Reynolds stresses and the mean rate of strain, which for the pure strain field (3.1), (3.2) becomes

$$-2\alpha\int\int uvdxdy. \quad (3.10)$$

This is zero for any flow symmetric about the x- or y-axis, as is the steady vortex described in Moore and Saffman (1971).

What will be the energy exchange if we suppose that an initially circular lens is subjected to a steady strain? We would expect the lens to adjust to the steady form found in section 4, such that it is elongated in the x-direction.

During the adjustment process, there will be a net outflow along the x-axis, and net inflow along the y-axis. The integrand on the right of (3.9) will thus be negative, suggesting that the lens will lose energy to the strain field during adjustment.

We thus speculate that, upon encountering strain, an initially circular lens will distort with its long axis along the outflow of the strain, due to the kinematic effect of the mean velocity. It will then precess so that its long axis is 45° to the principal axis of the strain, as shown in Fig. 2, and the loss of energy will stop.

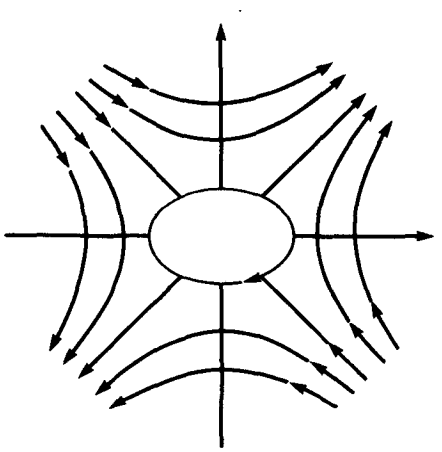

FIG. 2. Sketch of an elliptical lens in a pure strain field, oriented so that there will be no energy exchange between the lens and the flow in the layers above and below the lens.

4. Elliptical lenses in a pure straining motion

We now look for lenslike solutions of (3.3)–(3.5) with uniform rotation at angular rate Ω (vorticity 2Ω), expected to be negative for an anticyclonic lens, and ellipse parameter ϵ. The ellipse parameter ϵ is related to the ratio of major/minor axes r by

$$r^2=\left[\frac{x\text{-axis}}{y\text{-axis}}\right]^2=\frac{1-\epsilon}{1+\epsilon}.$$

The major axis is aligned with the y-axis for $\epsilon > 0$. The lens velocities and thickness will take the form

$$u=-\Omega(1-\epsilon)y \quad (4.1)$$
$$v=+\Omega(1+\epsilon)x \quad (4.2)$$
$$h/H_0=1-\mathrm{Bu}R_d^{-2}\{(1+\delta)x^2+(1-\delta)y^2\}. \quad (4.3)$$

Here, δ is the ellipse parameter of the h-contours, and H_0 the central thickness of the lens. The internal radius of deformation is $R_d = (g'H_0)^{1/2}/f$, and the Burger number Bu, a measurement of lens radius, will be determined. These solutions are similar in form to, and were motivated by, the nonsteady solutions for anticyclonic lenses in zero mean flow of Cushman-Roisin (1984) and Cushman-Roisin et al. (1985).

Substituting (4.1)–(4.3) into (3.5) gives $\epsilon = \delta$, which says that streamlines and height contours must coincide, a consequence of the uniform vorticity and conservation of potential vorticity for all fluid elements in the lens. Substitution into (3.3) and (3.4) gives

$$\Omega^2(1-\epsilon^2)+\Omega f(1+\epsilon) + 2f^2\mathrm{Bu}(1+\epsilon)+\alpha^2-\alpha f=0 \quad (4.4)$$

$$\Omega^2(1-\epsilon^2)+\Omega f(1-\epsilon) + 2f^2\mathrm{Bu}(1-\epsilon)+\alpha^2+\alpha f=0. \quad (4.5)$$

The sum and difference of these equations yield

$$\Omega^2(1-\epsilon^2)\epsilon+\alpha f+\alpha^2\epsilon=0 \quad (4.6)$$

$$2\ \mathrm{Bu}=\alpha/\epsilon f-\Omega/f. \quad (4.7)$$

The approach taken will be to regard Ω and α as fixed, and solve (4.6) as a cubic in ϵ. Once ϵ is known, we solve (4.7) for Bu. The three (i = 1 to 3) roots for ϵ are given by

$$\epsilon=\begin{cases} A+B \\ \dfrac{-A+B}{2}\pm(-3)^{1/2}\dfrac{A-B}{2} \end{cases} \quad (4.8)$$

where

$$A=(S/2W^2+\sqrt{Q})^{1/3}$$
$$B=(S/2W^2-\sqrt{Q})^{1/3}$$
$$Q=(S/2W^2)^2-(1+S^2/W^2)^3/27$$
$$S=\alpha/f$$
$$W=\Omega/f.$$

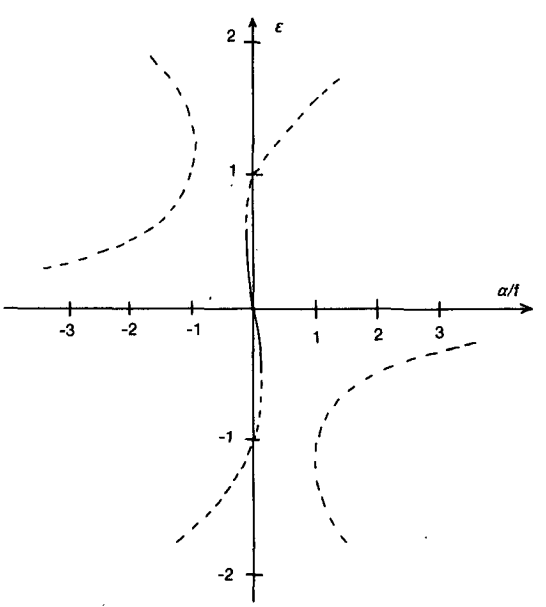

FIG. 3. Plot of Eq. (4.6) for a lens Rossby number ($2\Omega/f$) of 1. The solid portion of the central curve has physical relevance to anticyclonic lenses.

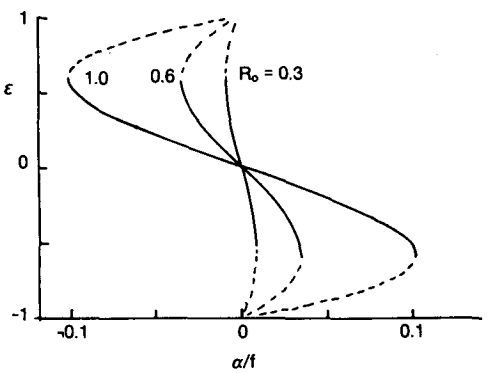

FIG. 4. Plot of Eq. (4.6) in more detail for three values of the Rossby number.

These are shown in Fig. 3, a plot of ϵ versus α/f for $\Omega = -f/2$, a Rossby number of 1. [The curves were actually plotted by regarding (4.6) as a quadratic in α.] Only the solid portion has direct physical relevance to anticyclonic lenses, showing a circular lens that becomes more elliptical with increasing strain. For positive strain, the ellipse parameter is negative, so the ellipse and strain are oriented as shown in Fig. 2a. Reversing the sign of the strain gives positive ellipse parameter, equivalent to Fig. 2a being rotated by 90°.

The physically relevant root is shown in more detail in Fig. 4, for Rossby number $\mathrm{Ro} = 2\Omega/f = 0.3$, 0.6 and 1. It is seen that the ellipse parameter increases with increasing strain, but beyond some maximum strain, given by $Q = 0$ above,

$$\frac{27}{4}W^2S^2=(W^2+S^2)^3 \quad (4.9)$$

there are no real solutions for ϵ, and hence no steady lenslike solutions of the form assumed. In the solid curve of Fig. 5 this maximum strain is plotted as a function of the lens rotation rate (half the Rossby number), showing that no lens of the form assumed can survive a strain rate exceeding $0.1f$. The ellipse parameter at this maximum strain is shown as the solid curve in Fig. 6; the maximum ellipse parameter is almost independent of the lens vorticity.

For a barotropic vortex ($f = 0$) in strain, Moore and Saffman (1971) found that the vortex became elliptical, with the same orientation to the strain axis that we found (for negative vorticity). In our notation, the equivalent relation to (4.6) was found by Moore and Saffman to be

$$\frac{\alpha}{\Omega}=-\epsilon\frac{1-\epsilon^2}{1+\epsilon^2}. \quad (4.10)$$

This allows solutions up to a maximum strain of $\alpha \sim 0.075\Omega$ at a maximum ellipse parameter of about 0.49. These maxima are shown in Figs. 5 and 6, respectively.

The changes in lens shape as the strain increases from zero to the critical value are shown in Fig. 7, as

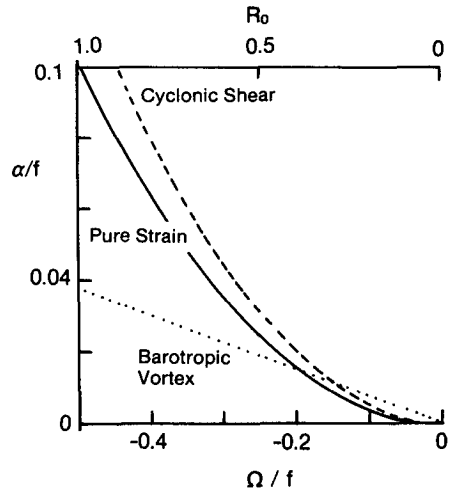

FIG. 5. Plot of the maximum strain or shear allowed in the solution versus the lens rotation rate, for a lens in pure strain (solid curve), simple shear (dashed curve), and a barotropic vortex in pure strain (dotted line, from Moore and Saffman, 1971).

the deformation radius divided by the lens dimensions. The inverse lens radius ($Bu^{1/2}$) at zero strain is shown as a function of Ω/f by the dashed line. The maximum corresponds to the smallest lens radius of $\sqrt{8}$ deformation radii. The central solid line is the same quantity, $Bu^{1/2}$, at the maximum strain shown in Fig. 5. The upper and lower solid curves are the corresponding inverse semiminor and semimajor axes. Lenses with even a moderate rate of spin have average radius less than 5 deformation radii. The shape of a lens at maximum strain is shown in Fig. 2a.

5. Elliptical lenses in simple shear flow

For a simple shear, $\bar{u} = \gamma y$, the equations of motion for the central layer (2.2)–(2.4) become

$$\frac{du}{dt} - fv = -g'\frac{\partial h}{\partial x} \tag{5.1}$$

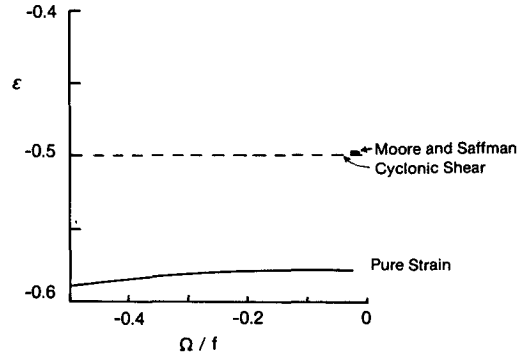

FIG. 6. Plot of the lens ellipse parameter at the maximum strain for the three cases described in Fig. 5.

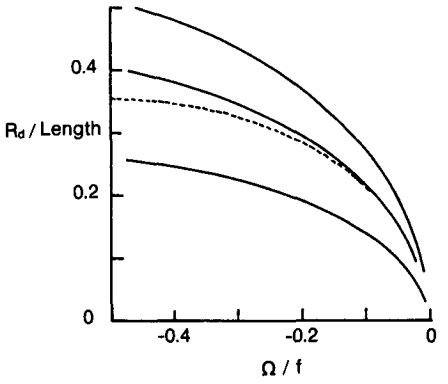

FIG. 7. Inverse lens dimension, normalized by the deformation radius, for the solutions of section 4. The solid curves are, top to bottom, the minimum, average and maximum radii for a lens at the maximum strain allowed for the lens versus the lens Rossby number. The dashed curve is the radius of the lens at zero strain versus Rossby number.

$$\frac{dv}{dt} + fu = -g'\frac{\partial h}{\partial y} + \gamma f y \tag{5.2}$$

$$\frac{dh}{dt} + h\left(\frac{\partial u}{\partial x} + \frac{\partial v}{\partial y}\right) = 0. \tag{5.3}$$

The energy equation analogous to (3.8) is

$$\frac{\partial}{\partial t}(\text{Energy}) = \gamma f \int\int yhv\,dx\,dy. \tag{5.4}$$

The elliptical lens solutions (4.1)–(4.3), when substituted into (5.1)–(5.3), give

$$\Omega^2(1-\epsilon^2) + \Omega f(1+\epsilon) + 2f^2\,\text{Bu}(1+\epsilon) = 0 \tag{5.5}$$

$$\Omega^2(1-\epsilon^2) + \Omega f(1-\epsilon) + 2f^2\,\text{Bu}(1-\epsilon) + \gamma f = 0, \tag{5.6}$$

and these can be solved to obtain the lens ellipse parameter and size in terms of the shear:

$$\frac{\gamma f}{\Omega^2} = -2\epsilon(1-\epsilon) \tag{5.7}$$

$$2\,\text{Bu} = -\Omega/f - (\Omega^2/f^2)(1+\epsilon). \tag{5.8}$$

Equation (5.7) is sketched in Fig. 8, showing that the relation between strain and ellipse parameter (a parabola) is not antisymmetric as we found for a pure strain. Rather, cyclonic and anticyclonic shear affect the lens differently.

For positive γ (anticyclonic shear), the ellipse parameter is negative, becoming -1 at a shear of $4\Omega^2/f$. As shown in Fig. 9a, this represents a lens stretched out parallel to the shear, becoming infinitely thin in this limit.

For negative γ (cyclonic shear), the ellipse parameter is positive, representing a lens stretched out with its long axis *across* the shear, as shown in Fig. 9b. As found in section 4 for pure strain, there is a maximum allowed cyclonic shear of $\Omega^2/(2f)$, at which $\epsilon = 0.5$, and beyond

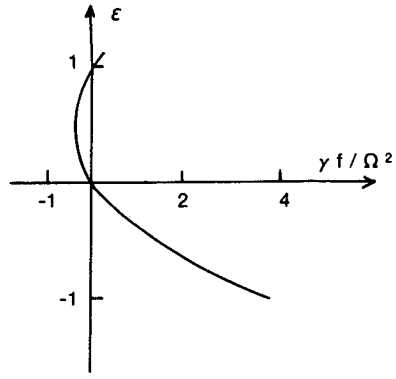

FIG. 8. Eccentricity of a lens in simple shearing flow versus the nondimensional rate of shear.

which solutions of the assumed form do not exist. This maximum shear is the dashed curve in Fig. 5 and is seen to be not very different from the maximum strain found in section 4. The ellipse parameter at the maximum shear is shown in Fig. 6, for comparison with the pure strain counterpart.

The principal axes of the pure strain component of the shear flows are also shown as dashed lines in Fig. 9. It is seen that the lens is oriented with its major axis 45° clockwise from the strain axis, as found in section 4. Thus, it seems that the strain is the primary agent causing the deformation of the lens. We expect that the vorticity of the mean flow mostly affects the Burger number of the lens. Assuming a mean flow consisting of solid body rotation confirms this; the ellipse parameter is zero, and only the size of the lens is affected.

This solution for a lens in a simple shearing flow is an extension to finite shear of the solution by Nof (1985). Nof assumed $\gamma/\Omega \ll 1$ and allowed for a mean advection velocity in addition to the shearing flow. For small γ, (5.7) becomes $\epsilon = -\gamma f/2\Omega^2$, and this agrees with Nof's result. The novel result here is the finding that the solution does not exist beyond a certain value of cyclonic shear, and that cyclonic and anticyclonic shear affect the lens differently.

6. Geostrophic adjustment in shear flow

In this section we investigate the adjustment of a long thin strip of fluid, initial thickness H_0 and initial width $2y_0$, in a shear flow $\bar{u} = \gamma y$. The strip is oriented parallel to the mean flow, along the x-axis. It is found that the shear modifies the width, but not the shape of the adjusted layer, and imposes no upper limit on the strength of the shear, other than f.

For the simple shear flow described, Eqs. (5.1)–(5.3) describe the evolution of the layer. From section 3, potential vorticity of the layer is conserved and is equal to f/H_0. Thus, assuming the adjusted layer to depend only on y and have $v = 0$:

$$\frac{\partial u}{\partial y} = f[1 - h(y)/H_0]. \tag{6.1}$$

Equation (5.1) becomes degenerate for the steady state and is not used. Equations (6.1) and (5.2) give

$$\left(R_d^2 \frac{\partial^2}{\partial y^2} - 1\right)\frac{h}{H_0} = \frac{\gamma}{f} - 1, \tag{6.2}$$

and u may be obtained from h trivially via (5.2). The solution, with boundary conditions $h = 0$ at $y = \pm y_1$, and y_1 to be determined later, is

$$\frac{h}{H_0(1-\gamma/f)} = 1 - \frac{\exp\{-(y+y_1)/R_d\} + \exp\{(y-y_1)/R_d\}}{1 + \exp\{-2y_1/R_d\}}. \tag{6.3}$$

Since the volume of the layer is conserved during adjustment, y_1 is determined by

$$\int_0^{y_1} h\,dy = y_0 H_0, \tag{6.4}$$

which gives a transcendental equation for y_1:

$$\frac{y_0}{1-\gamma/f} = y_1 - R_d \tanh(y_1/R_d). \tag{6.5}$$

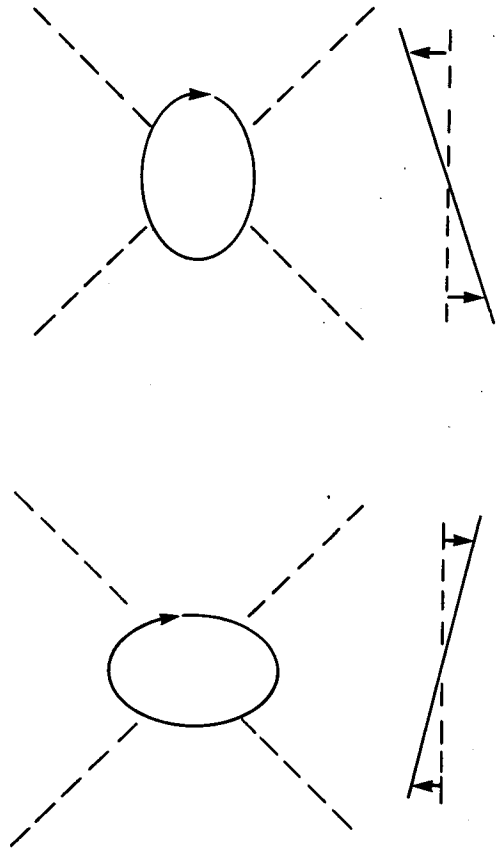

FIG. 9. Sketch of a lens in simple shearing flow. (a) Anticyclonic, for which the lens is aligned with the flow. (b) Cyclonic, for which the lens is aligned across the flow.

This relation is plotted in Fig. 10. Adjustment is generally outward and is accentuated by anticyclonic shear. Cyclonic shear inhibits outward adjustment and can even force inward adjustment. The only apparent limit to the shear is $\gamma = f$ for anticyclonic shear, at which the adjusted size becomes infinite. The reason for this behavior is related to the zones of strong anticyclonic vorticity produced by vortex squashing at the outer edges. At these points the vorticity approaches $-f$, and the velocity approaches $(g'H_0)^{1/2}$, forming a "buffer zone" that resists the effects of shear flow.

What are the differences between the adjustment model in this section and the elliptical lens of section 5? The assumption of constant potential vorticity in this model leads to a different velocity profile, vorticity at the edge equal to $-f$ (generally larger than for section 5), and vorticity at the center equal to $-f\,\mathrm{sech}(R_d/y_1)$ (generally smaller than the same size lens in section 5). The assumption of infinite length is very unrealistic, so the implications of this model are far from clear.

Discussion

a. Summary

We have examined the behavior and the survival of an isolated anticyclonic lens in large-scale straining and shearing flows. By means of a three-layer model in which we allow one baroclinic mode (the lens) and a barotropic large-scale flow, we studied a particular exact, nonlinear solution representing a steady elliptical lens with uniform interior vorticity. This lens becomes increasingly elliptical in response to increasing strain or shear. In pure strain, the major axis of the lens is 45° clockwise from the principal strain axis, as shown in Fig. 2a. In a simple shear flow, the lens lies with its major axis parallel to anticyclonic shear and perpendicular to cyclonic shear, as shown in Fig. 9. When the simple shear is decomposed into strain plus rotation, the major axis lies 45° clockwise from the principal strain axis, as for pure straining motion. This orientation is one in which there is no energy exchange between the lens and the mean flow, thus allowing a steady state.

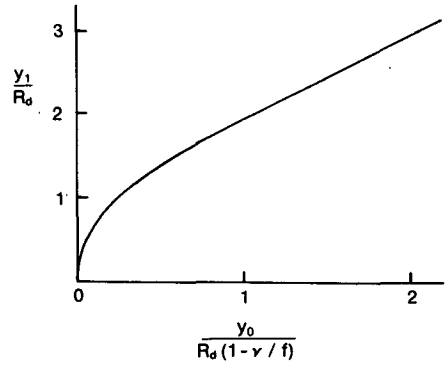

FIG. 10. Solution of the transcendental equation (6.5), giving the adjusted lens width, y_1, as a function of the initial lens width, y_0.

As the strain increases to the value given in (4.9), the ellipse parameter increases to a maximum value (about 1/2). No steady solutions of the form assumed exist for strain larger than this value. Cyclonic shear causes similar behavior (section 5), with a maximum shear beyond which solutions do not exist. Anticyclonic shear does not cause this maximum. As the shear increases, the lens becomes more and more elliptical, becoming infinitely long and thin as the shear approaches $-f$. In this case the alignment of the lens with the shear flow reduces the importance of the advective terms, allowing the lens to persist in stronger shear.

b. Model shortcomings

The rather simple model used here has several unrealistic facets, some more serious than others. Neglect of friction and mixing is not likely to be serious, since these effects occur on time scales of at least several months, compared to the time scale of several days for adjustment of the lens to a change in the strain field. As discussed in McWilliams (1985), ambient potential vorticity gradients can have subtle effects. Unless the lens has zero net angular momentum (which seems unlikely considering the probable generation by collapse and geostrophic adjustment), the lens must radiate momentum and energy in the form of Rossby waves. The effects of this radiation are, however, felt on rather long time scales, allowing their neglect here.

The more serious deficiencies of the model have to do with the reduced number of degrees of freedom in the vertical and horizontal description of the lens. The three-layer model only allows one baroclinic and one barotropic mode and thus neglects any back effects that the lens has on the mean flow. The extreme vortex squashing at the lens edge where the thickness approaches zero requires that either the vorticity approach $-f$ or the potential vorticity approach infinity at the rim. Neither possibility seems very realistic; the model used here assumes the latter. Another simplification of the model is the assumption of uniform vorticity, which implies a particular radial distribution of velocity, vorticity and potential vorticity. The radial degrees of freedom are, in effect, reduced from infinity to one, and the lens Burger number is constrained to be a function of the Rossby number. This shape can be defended only by noting that observed lenses have a central region of uniform vorticity and that observed lens thicknesses fall off as r^2 (Armi and Zenk, 1985).

An alternate three-layer model would be to assume (in the spirit of Csanady, 1979, and Flierl, 1979) that the water within the lens has uniform potential vorticity f/H_0, as if the lens had adjusted geostrophically to a steady state from an initial thickness H_0. The set of

equations to solve would then be the two momentum equations (3.3) and (3.4), together with the first integral of the expression of conservation of potential vorticity, (3.6):

$$\frac{\partial u}{\partial y}-\frac{\partial v}{\partial x}=f(1-h/H_0). \tag{7.1}$$

The conservation of lens volume, (3.7), would enter in as an a posteriori constraint to determine the position of the lens edge. The most unrealistic feature of the solution to this problem (not found in observed lenses) is the strong vorticity and velocity near the rim, where the thickness vanishes. This "high-speed buffer zone" may artificially protect the interior of the lens from the effects of a strong strain field, allowing it to persist in a much larger strain than predicted by the model in section 4. This seems to be the case for the "infinite strip" model in section 6. The most unrealistic feature of this kind of model is the infinitely large gradient of potential vorticity at the lens edge, which continuous stratification and diffusion would smooth out.

It appears that the major problem with the model is the choice of a particular, possibly unrealistic, radial distribution of velocity. In real lenses this distribution is determined by the generation mechanism of the lens, the lateral stirring of fluid columns within the lens (which homogenizes potential vorticity), and any friction effects, which act to diffuse velocity gradients and so promote solid body rotation. The stirring and mixing effects would certainly prevent the infinite radial gradients found in the earlier models. Even given a realistic model of the radial structure of a lens, there is no guarantee it will allow analytic solutions, as has the uniform vorticity model.

c. *Some speculations*

What happens to a lens if the external flow field is increased beyond the point that allows steady solutions? There are at least three possibilities.

1) The lens may readjust (in a manner consistent with potential vorticity conservation) to a steady velocity distribution and shape other than the one assumed.

2) The lens may remain a coherent entity, but with unsteady form. Examples of such unsteady finite-amplitude solutions for the case of zero-external flow are the oscillatory modes of a solitary vortex discovered by Cushman-Roisin (1984) and Cushman-Roisin et al. (1985).

3) The lens may break up.

The limited horizontal description of the lens profile in the present model seems to preclude analytic investigation of the first possibility. The second possibility, and to a limited extent, the third, is being studied by a generalization of the nonlinear, time-dependent model of Cushman-Roisin et al. (1985). Finally, the stability of these profiles to lens breakup is being addressed by perturbation analysis. In what follows, we speculate that the lens breaks up in response to large shear or strain fields.

The various models imply that a lens with a given central vorticity (or Rossby number) should only be able to withstand a certain environmental strain before something drastic occurs. The value of this strain depends on the detailed velocity profile of the lens, but should be close to one of the curves in Fig. 5. If this strain is exceeded, the lens is likely to be torn apart by the strain, losing material from its edge. The remaining core of the lens will now be much smaller in radius; the lens Burger number is larger, but the Rossby number is the same. The lens will now collapse, becoming a little thinner and larger in diameter and spinning a little faster. The Burger number will become smaller and the Rossby number larger. With a larger Rossby number the lens should now be more resistant to being torn apart by the strain field. The net result is that one should only tend to see lenses strong enough to survive a strain rate they are likely to encounter. Such encounters only make the lenses smaller and more intense. During these encounters, the maximum ellipse parameter should be 0.58 (a 2:1 major/minor axis ratio). Between such encounters, the effects of friction and Rossby wave radiation would weaken the lenses.

From Fig. 2 of Colin de Verdiere et al. (1985), a typical rate of strain due to the mesoscale eddy field in the eastern North Atlantic is in the range $\alpha/f = 0.013$–0.04. From Fig. 5, this translates to a Rossby number in the range 0.3–0.7. This implies that we should not expect to see many lenses with Rossby number less than this. The lenses described by Armi and Zenk (1985) have a velocity maximum of about 30 cm s^{-1} at a radius of about 30 km, corresponding to a Rossby number of about 0.3. The few lenses that migrate to the western basin have virtually no chance of surviving the return trip via the Gulf Stream, since the shear in the Stream is quite strong: $\gamma/f \sim o(1)$. In their survey of intrathermocline lenses, Dugan et al. (1982) found no lenses in the Gulf Stream outflow region between 40° and 42°N. The effects of large-scale strain on lenses would suggest that they should become progressively smaller and fewer from east to west and that none should survive the return trip in the Gulf Stream.

Acknowledgments. I thank John Middleton for stimulating discussions that initiated this research and for pointing out the stress/strain energy exchange relation (3.10) for nonrotating flow. Thanks to Dave Hebert, Jim McWilliams, and Benoit Cushman-Roisin for their constructive comments on the manuscript. My research is supported by the Natural Sciences and Engineering Research Council of Canada.

REFERENCES

Armi, L., and W. Zenk, 1985: Large lenses of highly saline Mediterranean Water. *J. Phys. Oceanogr.*, **14,** 1560–1576.

Colin de Verdiere, A. C., J. G. Harvey and M. Arhan, 1985: Stirring and mixing of mesoscale thermohaline anomalies. Submitted to *J. Mar. Res.*

Csanady, G. T., 1979: The birth and death of a warm-core ring. *J. Geophys. Res.*, **84,** 777–780.

Cushman-Roisin, B., 1984: An exact analytical solution for a time-dependent, elliptical warm-core ring with outcropping interface. *Ocean Modelling,* **59,** 5–6.

——, W. H. Heil and D. Nof, 1985: Oscillations and rotations of elliptical warm-core rings. *J. Geophys. Res.*, **90,** 11 756–11 764.

Dugan, J. P., R. P. Mied, P. C. Mignery and A. F. Schuetz, 1982. Compact, intrathermocline lenses in the Sargasso Sea. *Geophys. Res.*, **87,** 385–393.

Flierl, G. R., 1979: A simple model for the structure of warm and cold core rings. *J. Geophys. Res.*, **84,** 781–785.

McDowell, S., and T. Rossby, 1978: Mediterranean Water: An intense mesoscale eddy off the Bahamas. *Science,* **202,** 1085–1087.

McWilliams, J. C., 1985: Submesoscale, coherent vortices in the ocean. *Rev. Geophys.*, **23,** 165–182.

Moore, D. W., and P. G. Saffman, 1971: Structure of a line vortex in an imposed strain. *Aircraft Wake Turbulence* Olsen, Goldburg and Rogers, Eds., Plenum, 339–354.

Nof, D., 1985: On the ellipticity of isolated anticyclonic eddies. *Tellus,* **37A,** 77–86.

Pedlosky, J., 1979: *Geophysical Fluid Dynamics,* Springer-Verlag, 624 pp.

Rossby, T., 1982: *Eddies in Marine Science,* A. R. Robinson, Ed.

Tennekes, H., and J. L. Lumley, 1972: *A First Course in Turbulence,* MIT Press, 300 pp.